Nuclear Data for Science and Technology (1988 MITO), 249- 252, Copyright © 1988 JAERI.

# CROSS SECTIONS FOR THE NEUTRON-INDUCED REACTIONS ON $^{6}Li$ AND $^{7}Li$ AT 14.1 MEV

Shoji Shirato, Shinji Shibuya and Yoshiaki Ando
Department of Physics, Rikkyo (St. Paul's) University,
Nishi-Ikebukuro, Toshima-ku, Tokyo 171, Japan
and
Keiichi Shibata
Japan Atomic Energy Research Institute,
Tokai-mura, Ibaraki-ken 319-11, Japan

Abstract: A summary of our recently and previously measured cross sections for 14.1 MeV neutron-induced reactions on lithium isotopes has been presented. These data of measurements of charged particles except protons are also compared with available data of other authors. Our data were taken with a counter telescope consisting of two gas proportional counters and silicon ΔE and E detectors. Measured energy spectra of deuterons and tritons from the three-body break-up reactions $^{6}Li(n,d)^{5}He$ and $^{7}Li(n,t)^{5}He$, respectively, were analyzed by a simple final state interaction theory. Measured angular distributions for the above reactions as well as $^{6}Li(n,t)^{4}He$ and $^{7}Li(n,d)^{6}He$ were analyzed by DWBA calculations.

(nuclear reactions, $^{6,7}Li(n,d)$, $^{6,7}Li(n,t)$, E=14.1 MeV, measured σ(θ), DWBA)

## Introduction

Experimental data on the fast-neutron induced reactions of emission of charged particles from lithium isotopes $^{6,7}Li$ are very important for investigations of not only the reaction mechanism and the cluster structure in nuclear physics but also the fusion reactor in nuclear engineering. However, these data are very scarce at the present time.

Previously, we measured the differential cross sections for the reactions $^{6}Li(n,d)^{5}He$ and $^{6}Li(n,t)^{4}He$ at 14.1 MeV in a limited angular region and compared our data with the exact finite-range distorted wave Born approximation (EFR-DWBA) calculations[1]. Since then we have continued to take the data on not only $^{6}Li$[2,3] but also $^{7}Li$[4] without publication. Our $^{6}Li$ data are in agreement with the Zagreb data of 14.4 MeV[5-7], but are not reproduced at around 60° for (n,d) and at very backward angles for (n,t) by the EFR-DWBA calculations. Regarding our preliminary data[4] on the $^{7}Li(n,t)^{5}He$ reaction, which are also in fair agreement with the Zagreb data[6], it was difficult to reproduce even the shape of the measured angular distribution by EFR-DWBA calculations.

In this paper, we present a summary of our experimental data on the one- or two-nucleon transfer reactions for $^{6,7}Li$, and also describe the details of our newly performed experiments in the following section.

## Experimental procedures

The procedures of our experiments using 95.58% enriched $^{6}Li$ metal targets of various thicknesses of 2.35 - 3.74 mg/cm$^2$ and a preliminary one using a 12.44 mg/cm$^2$ natural lithium metal target have been reported in previously published[1] and unpublished[2,3,4] papers. These experiments have been performed using an old Cockcroft-Walton accelerator of the Rikkyo University. Here, we describe only our recent experiments on $^{7}Li$, in which a new 300 kV Cockcroft-Walton accelerator was used for the production of $^{3}H$-d neutrons of 14.1 MeV.

The absolute determination of the neutron yield in this experiment was done with an accuracy of about 2% by use of the "associated α-particle method" using a Si p-i-n photodiode (Hamamatsu S1723-06) as the α-monitor and a $^{3}H$-Ti-Cu target (Amersham TRT-31, 2.4 Ci). The details of this method are described elsewhere[8]. Another Si p-i-n photodiode (Hamamatsu S1722) and a NE213 liquid scintillator, which were placed at 3 cm and 100 cm respectively from the neutron source point, were employed as neutron detectors. An accelerated deuteron beam of 170 keV was collimated by passing through two collimators of 3 mm and 2 mm in diameter after forcusing by Q-magnets.

A 4.54 ± 0.14 mg/cm$^2$ target of 99.988% enriched $^{7}Li$ metal was prepared by rolling and placed at the center of a scattering chamber[9]. In the chamber, two counter telescopes (CT1 and CT2) were placed at 4 cm from the lithium target, where a collimator of 6 mm in diameter was located for defining each telescope aperture as seen in Fig. 1. Each counter telescope consists of two gas proportional counters and Si ΔE and E detectors. The counter gas of Ar with 5% of

$CO_2$ was filled to a pressure of 100 Torr in the chamber. The experimental arrangement is shown schematically in Fig. 1.

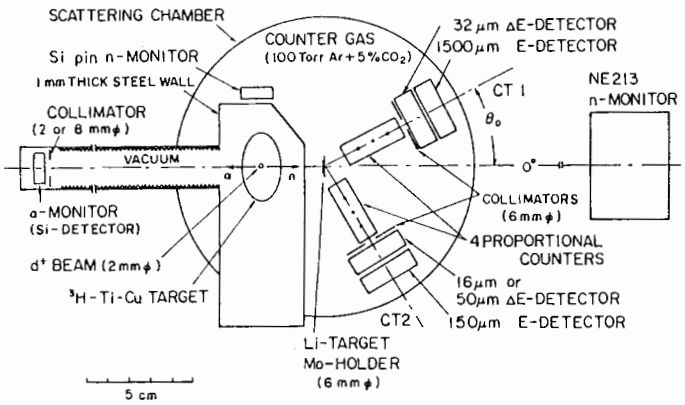


Fig. 1. Experimental layout.

Energy and time signals from eight detectors, viz. two counters ($PC_{11}$, $PC_{12}$) and 32 and 1500 μm Si detectors ($Si\Delta E_1$, $SiE_1$) for CT1, and two counters ($PC_{21}$, $PC_{22}$) and 50 and 150 μm Si detectors ($Si\Delta E_2$, $SiE_2$) for CT2, were taken as list mode data on magnetic tape by a CAMAC data acquisition system, after being treated by a NIM -module electronic system. The multiparameter event data were analyzed in real-time for the particle identification and energy spectra of identified charged particles (p, d, t or $^4$He) were obtained in off-line. The particle identification was almost completely performed.

The absolute cross sections for $^6$Li have been determined with overall accuracies of about ±5 - 11% for the (n,d) case and ±7 - 14% for the (n,t) case in a measured angular region from 0° to 130°. These uncertainties include the systematic error originated from the uncertainties in target thickness (±1 - 3%), geometry (±3%) and neutron flux (±1 - 2%). The absolute cross sections for $^7$Li were determined with the statistical errors of about ±4 - 32% for (n,t) in a measured angular region from 0° to 90° and of about ±40% for (n,d) in a measured region 0° - 50°. These data on $^7$Li do not include the systematic error mentioned above.

## Results and discussion

The energy spectra of deuterons and tritons from the reactions $^6$Li(n,d)$^5$He and $^7$Li(n,t)$^5$He, respectively, were measured at various telescope setting angles in the ranges from 0° to 130° for $^6$Li and to 90° for $^7$Li. A typical example of the measured spectra is shown in Fig. 2. The energy spectra observed at forward angles show remarkable peaks due to the final-state interaction (FSI) especially at the high energy end, as seen in Fig. 2. The curves drawn in Fig. 2 are the results of calculations taking into account n-α, n-t and t-α FSIs, which are represented by the phase-shifts $\delta^{2J}{}_L$ of L-wave scattering in the unobserved pair subsystem of total angular momentum J in the final state. An energy resolution of 800 keV has been folded into the curves of Fig. 2. Both the deuteron- and the triton-energy spectra are dominated by the FSI effects of the well-known $P_{3/2}$ n-α scattering at the high energy end. In this energy region, the Lehman effect of the n-α plane-wave final-state component[10] does not appear to be significant. In the case of the triton energy spectrum, the significant enhancement due to the t-α FSI appears in the middle energy region, as seen in Fig. 2. The corresponding d-α FSI enhancement in the case of the deuteron energy spectrum should exist in an unobserved low-energy region. Thus, in the case of the reaction consisting of three particles in the final state, the measured energy spectrum must be analyzed for each FSI channel in a three-body model and also corrected for any unobserved low-energy part, before energy integration of the double differential cross section obtained is carried out, in order to compare the experimental result with DWBA calculations.

The measured and analyzed data on the differential cross section for the $^6$Li(n,d)$^5$He ($P_{3/2}$) reaction in the center-of-mass (c.m.) system are summarized in Fig. 3 and also Table 1. The data[1] at each angle has been obtained from the measured energy spectrum by making a correction for the unobserved lower-energy region on the basis of the Watson-Migdal form. The curve drawn in Fig. 3 is the result of the EFR-DWBA

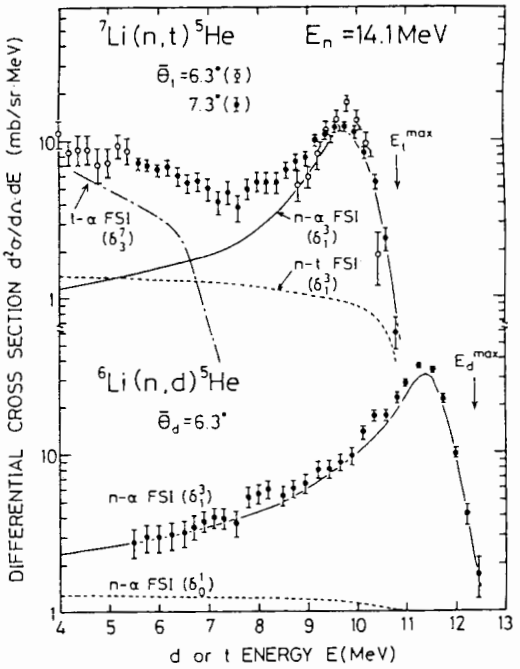


Fig. 2. Typical examples of measured and calculated deuteron- and triton-energy spectra.

calculation[1]. The sharp rise in the backward angular distribution predicting by the EFR-DWBA calculation is in favour of our data[3].

The measured data on the c.m. differential cross section for the $^{6}Li(n,t)^{4}He$ reaction are summarized in Fig. 4 and also Table 1. The curves in Fig. 4 are the result of the EFR-DWBA calculations in both cases of the incoherent sum of the deuteron-pickup amplitudes only (the solid line)[1] and the coherent sum between the d-pickup and the $^{3}He$-pickup amplitudes (the dashed line)[2].

The measured data on the c.m. differential cross section for the $^{7}Li(n,t)^{5}He$ reaction are shown in Fig. 5. The data[4] for $^{7}Li(n,t)^{5}He(P_{3/2})$ have been derived by the same way as that used in the case[1] of $^{6}Li(n,d)^{5}He(P_{3/2})$ without involving a plane-wave final-state component[10] in the n-α scattering state and some FSI channels other than the $P_{3/2}$ n-α channel. The curves in Fig. 5 are the result of the EFR-DWBA calculations.

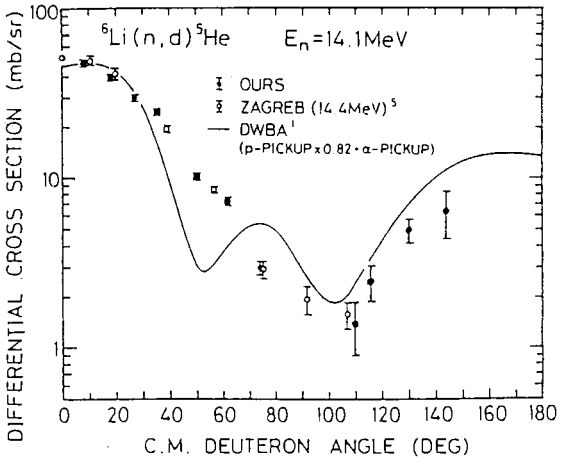


Fig. 3. Measured and calculated angular distributions of deuterons from the $^{6}Li(n,d)^{5}He$ reaction at 14.1 MeV.

Table 1. Measured c.m. differential cross sections for the reactions $^{6}Li(n,d)^{5}He$ and $^{6}Li(n,t)^{4}He$ at 14.1 MeV.

| Telescope setting angle $\theta_0$ (deg) | $^{6}Li(n,d)^{5}He$ C.m. mean angle $\theta_d$ *) (deg) | $^{6}Li(n,d)^{5}He$ $d\sigma(\theta_d)/d\Omega$ (mb/sr) | $^{6}Li(n,t)^{4}He$ C.m. mean angle $\theta_t$ (deg) | $^{6}Li(n,t)^{4}He$ $d\sigma(\theta_t)/d\Omega$ (mb/sr) | Ref. |
|---|---|---|---|---|---|
| 0 | 8 ± 5[a)] | 48.2 ± 2.4[b)] | 8 ± 4[a)] | 7.4 ± 0.5[b)] | 1 |
| 14 | 18 ± 8 | 39.3 ± 2.0 | 17 ± 8 | 5.5 ± 0.4 | 1 |
| 22 | 27 ± 8 | 30.0 ± 1.5 | 28 ± 9 | 2.7 ± 0.2 | 1 |
| 30 | 35 ± 7 | 24.6 ± 1.3 | 36 ± 7 | 2.1 ± 0.2 | 1 |
| 40 | 50 ± 6 | 10.2 ± 0.5 | 50 ± 7 | 2.0 ± 0.2 | 1 |
| 50 | 62 ± 6 | 7.3 ± 0.4 | 64 ± 6 | 1.5 ± 0.2 | 1 |
| 60 | 74 ± 5 | 3.0 ± 0.3 | 71 ± 5 | 1.3 ± 0.2 | 1 |
| 93 | 110 ± 5 | 1.4 ± 0.5 | 10 ± 5 | 1.8 ± 0.2 | 2 |
| 100 | 116 ± 4 | 2.5 ± 0.6 | 17 ± 4 | 1.7 ± 0.2 | 2 |
| 115 | 130 ± 4 | 5.0 ± 0.8 | 131 ± 4 | 1.4 ± 0.1 | 3 |
| 130 | 144 ± 3 | 6.4 ± 2.0 | 145 ± 3 | 1.7 ± 0.3 | 2,3 |
| 17 | | | 157 ± 9 | 1.3 ± 0.10[c)] | 1 |
| 11 | | | 165 ± 9 | 2.0 ± 0.14[c)] | 1 |
| 3 | | | 172 ± 6 | 2.3 ± 0.14[c)] | 1,2 |

The preliminary data on the c.m. differential cross sections for the reactions $^{7}Li(n,d)^{6}He(g.s.,0^{+})$ and $^{7}Li(n,d)^{6}He^{*}(1.80\ MeV,2^{+})$ are shown in Fig. 6. The measured cross section for $^{7}Li(n,d)^{6}He^{*}(1st)$ should be too large, because of the uncorrection for a contribution from $^{7}Li(n,d)\alpha 2n$. The final confirmation of the absolute cross sections is in progress. The curves drawn in Fig. 6 are the result of the EFR-DWBA calculation using the optical model potentials of Hyakutake et al.[11] for n-$^{7}Li$ and of Bingham et al.[12], who obtained the d-$^{6}Li$ potential, for d-$^{6}He$. All the DWBA calculations in this work were performed by using the code DWUCK5[13] and the potential parameters given in Table 2.

## Conclusions

The differential cross sections for the 14.1 MeV neutron induced reactions of charged particle emission from $^{6,7}Li$ were measured and summarized in this paper. Our experimental data are almost in agreement with the Zagreb data of 14.4 MeV.

Our data gave clear evidence of the backward increase of the $^{6}Li(n,d)^{5}He$ cross section, predicting by the EFR-DWBA calculation[1] based on the proton pickup mechanism. Generally, the EFR-DWBA calculations based on the pickup mechanism of one- or two-particle transfer reproduce forward differential cross sections for the (n,d)

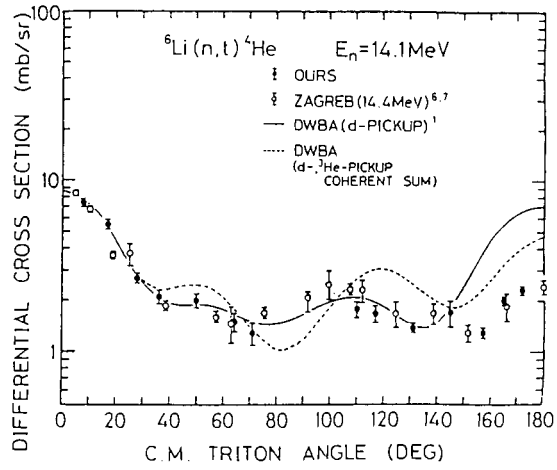


Fig. 4. Measured and calculated angular distributions of tritons from the $^{6}Li(n,t)^{4}He$ reaction at 14.1 MeV.

*) The angle corresponding to $^{5}He(g.s.)$.

a) HWHM of the calculated angular frequency distribution.

b) The error includes the systematic overall error (±4.8%) in addition to the statistical error.

c) The data from the alpha particle measurement.

and (n,t) reactions on $^{6}$Li. However, some discrepancies between the experimental data and the DWBA calculations appear over the whole angular region, especially at very backward angles. For example, a coherent sum of the d- and $^{3}$He-pickup amplitudes improves the discrepancy at larger angles than 150° for the $^{6}$Li(n,t) case. The experimental data on $^{7}$Li(n,t)$^{5}$He could be reproduced by only the d pickup mechanism or not the knock-on mechanism predicting too small cross sections. Further theoretical studies ar necessary to obtain better agreement with the experimental data.

This work has been supported in part by the Japan Atomic Energy Research Institute and by the Grant-in-Aid for General Scientific Research (No 62540214), the Ministry of Education in Japan.

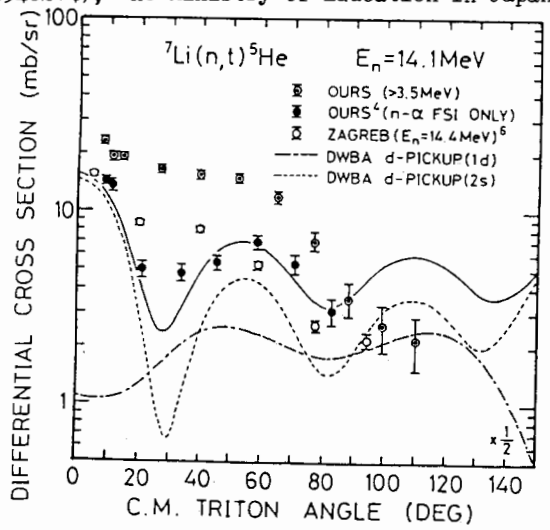


Fig. 5. Measured and calculated angular distributions of tritons from the $^{7}$Li(n,t)$^{5}$He reaction at 14.1 MeV.

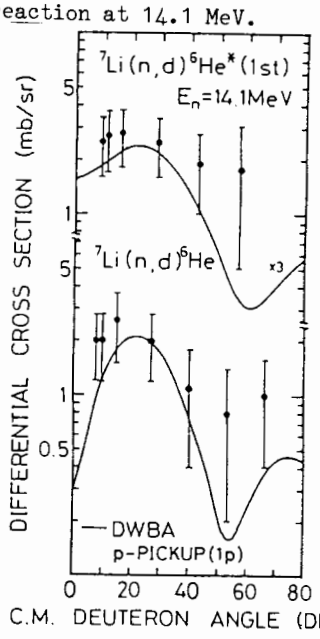


Fig. 6. Measured angular distributions of deuterons from the reactions $^{7}$Li(n,d)$^{6}$He(g.s.) and $^{7}$Li(n,d)$^{6}$He*(1st) at 14.1 MeV.

## REFERENCES


1. S. Higuchi, K. Shibata, S. Shirato and H. Yamada: Nucl. Phys. A384, 51(1982)
2. H. Yamada, Y. Ando and S. Shirato: JAERI Report 1983, NEANDC(J)-94/U, INDC(JAP)-81/U, p.75
3. Y. Ando, S. Shirato and H. Yamada: JAERI Report 1984, NEANDC(J)-104/U, INDC(JPN)-92/U, p.58
4. I. Furutate, T. Kokubu, Y. Ando, T. Motobayashi and S. Shirato: JAERI Report 1985, NEANDC(J)-116/U, INDC(JPN)-102/U, p.81; I. Furutate: Master thesis (Rikkyo University, 1986)
5. V. Valković, G. Paić, I. Slaus, P. Tomas, M. Cerineo and G.R. Satchler: Phys. Rev. 139, B331(1965)
6. V. Valković, I. Slaus, P. Tomas and M. Cerineo: Nucl. Phys. A98, 305 (1967)
7. D. Rendić and G. Paić: Rossendorf Reports 2, 143(1967)
8. S. Shirato, S. Shibuya and Y. Ando: RUP-88-1 (Rikkyo University Preprint, unpublished, 1988)
9. S. Shirato, K. Shibata, M. Saito and S. Higuchi: Nucl. Instr. Meth. 199, 469(1982)
10. C.T. Christou, D.R. Lehman and W.C. Parke: Phys. Rev. 37, 445, 458(1988)
11. M. Hyakutake, M. Sonoda, A. Katase, Y. Wakuta, M. Matoba, H. Tawara and I. Fujita: J. Nucl. Sci. Technol. 11, 407(1974)
12. H.G. Bingham, A.R. Zander, K.W. Kemper and N.R. Fletcher: Nucl. Phys. A173, 265(1971)
13. P.D. Kunz: University of Colorado Report, unpublished


Table 2. Potential parameters used in the EFR-DWBA calculations.

| | n-$^{6}$Li | n-$^{7}$Li | d-$^{5}$He | t-$^{4}$He | t-$^{5}$He | d-$^{6}$He |
|---|---|---|---|---|---|---|
| V (MeV) | 37.3 | 37.0 | 115.0 | 138.0 | 138.0 | 92.5 |
| W (MeV) | 19.2$^{G}$ | 19.0$^{G}$ | 0.68$^{S}$ | 2.0$^{V}$ | 2.0$^{V}$ | 72.4$^{S}$ |
| $V_{so}$(MeV) | 31.2 | 18.8 | 0.0 | 9.2 | 18.8 | 17.2 |
| $r_0$ (fm) | 1.63 | 1.60 | 1.26 | 0.93 | 1.10 | 2.17 |
| $r_0'$(fm) | 1.43 | 1.43 | 1.80 | 2.00 | 2.00 | 2.35 |
| a (fm) | 0.53 | 0.50 | 0.73 | 0.70 | 0.70 | 0.61 |
| b (fm) | 0.55 | 0.40 | 0.31 | 0.65 | 0.65 | 0.61 |
| $r_c$ (fm) | 0.00 | 0.00 | 1.40 | 1.40 | 1.40 | 1.40 |
| Ref. | 11 | 11 | 1 | 1 | | 12 |

G: Gauss, S: Surface W-S, V: Volume W-S.